 doi:10.20944/preprints201705.0057.v1

The Thermal Conductivities of Periodic Fibrous Composites as Defined by a Mathematical Model

John Venetis: School of Applied Mathematics and Physical Sciences NTUA, Email: johnvenetis4@gmail.com

Emilio Sideridis (Cor. Author): School of Applied Mathematics and Physical Sciences NTUA, Section of Mechanics, 5 Heroes of Polytechnion Avenue, GR – 15773 Athens, Greece.
Telephone: +302107721224 Fax: +302107721302 Email: siderem@mail.ntua.gr

Abstract

In this paper, an advanced geometric model to simulate the periodic structure of unidirectional fibrous composites is presented. This model takes into consideration the influence of fiber contiguity in parallel with the concept of interphase on the thermomechanical properties of the overall material. Next, by the use of this model the authors propose closed – form expressions to estimate the longitudinal and transverse thermal conductivity of this type of composites.

Keywords

fibrous composites; periodic structure; fiber contiguity; interphase; thermal conductivities

1. Introduction

To characterize fibrous composite materials, a great number of parameters are necessary. In particular, the physical behavior of the system depends on the fiber orientation and distribution, the matrix and on the fiber matrix interaction or adhesion. In fact, fiber reinforcement makes the composite strong. However, a disadvantage in fibrous composites is that the fibers are able to transmit loads only in the direction of their axis and unfortunately there is less strengthening effect in the direction perpendicular to the axis.
On the other hand, the role of the matrix is to protect the fiber from corrosive action of the environment and to ensure interactions amongst the fiber by mechanical physical and chemical effects. In the fibrous reinforced composites, the deformation of the matrix is then used to transfer stresses to the embedded high – strength fibers by means of shear tractions at the fiber matrix interface. Meanwhile, fibers retard the propagation of cracks and thus produce a material of high strength. To simulate the microstructure of such materials, a large number of models appeared in the literature. Some of them take into account the existence of an intermediate phase, developed during the preparation of the composite material and which plays an important role on the overall thermomechanical behavior of the composite.
In a model developed by Theocaris et al [1, 2] this intermediate phase has been considered initially as being a homogeneous and isotropic material. In a better approximation [3] a more complex model has been introduced, according to which the fiber was surrounded by a series of successive cylinders, each one of them having a different elastic modulus in a step-function variation with the polar radius.
Moreover, mathematical analyses of inhomogeneous interphases started, probably, with the work of Kanaun and Kudryavtseva [4] on the effective elasticity of a medium with spherical inclusions surrounded by radially inhomogeneous interphase zones. In this remarkable work, the basic idea of replacing an inhomogeneous inclusion by an equivalent homogeneous one was advanced. Such a replacement was carried out by modeling the inhomogeneous interface by a number of thin concentric layers (piecewise constant variation of properties). A similar analysis for cylindrical inhomogeneities (fibers) surrounded by concentric layers was carried out by the same authors [5]. Ideas of this work have appeared again in a number of later works. For instance, the basic idea of replacing inhomogeneous inclusions by equivalent homogeneous ones has been utilized in the majority of works on the topic; the idea of approximating radially variable properties by multiple layers (piecewise constant variation of properties) was suggested by Garboczi and Bentz [6] and Garboczi and Berryman [7] in the context of applications to concrete composites. Moreover, several explicit solutions for two specific forms of radial variation of properties, i.e. the linear and the power law ones, have been derived. Specifically, in Ref. [8] the linear variation of the thermal expansion coefficient for a large category of

composites was considered whereas in Refs. [9, 10] an implementation of the power law variation, in the context of effective bulk modulus and effective conductivity took place.
As far as an arbitrary law of radial variation in properties is concerned, the methodology was proposed by Shen and Li [11], whereby the thickness of the interface is increased in an incremental, "differential" manner, with homogenization at each step. This concept was modified in Refs. [12, 13]. In these works the effective thermoelastic properties of composite materials with coated inhomogeneities were computed, assuming arbitrary variation of the material properties across the interphase zone.
Meanwhile, for a detailed investigation on the influence of particle arrangement on the thermomechanical properties of particulate composites one may refer to [14, 15].
Besides, the most popular thermal conductivity models were initiated with the standard and inverse mixture law. The composite thermal conductivity in the fiber direction is estimated by the standard mixture rule, which constitutes the weighted average of filler and matrix thermal conductivities. This model is typically used to predict the thermal conductivity of a unidirectional composite with continuous fibers. In contrast, for the direction perpendicular to the fibers the series model which is also known as inverse law of mixtures is applicable to estimate thermal conductivity of a unidirectional continuous fiber composite [16, 17]. Furthermore, Hashin – Rosen cylinder assemblage model considers a transversely isotropic fiber reinforced cylinder in which the phases are transversely isotropic with material axes of symmetry in cylindrical axis direction [18]. The two phases of the composite are simulated as smooth and parametrized geometrical surfaces. This model gives the upper and lower bound for transverse thermal conductivity. Further, in Ref. [19] numerical calculations of the effective thermal conductivity of unidirectional fibrous composite materials with an interfacial thermal resistance between the continuous and dispersed components were carried out.
Finally, in Ref. [20] the thermal conductivity of homogeneous particulate composites of periodic structure was estimated by means of a mathematical model. This model took into consideration the particle distribution and contiguity together with the concept of interphase.
In the present work, the thermal conductivities of periodic fibrous composites are evaluated by means of three prismatic geometric models, the unit cells of which are transformed into a 7 – phase cylindrical model. The above mentioned body centered model takes into account the arrangement of internal and neighboring fibers via deterministic configurations and their contiguity, together with the concept of interphase on the thermomechanical properties of the composite.
In this context, the authors propose amended forms of the standard and inverse law of mixtures, in order to determine the longitudinal and transverse thermal conductivity of the overall material.

2. Simulation of fiber arrangement

As it is known, the majority of microstructural models which may concern either particulate or fiber composites aim at the reproduction of the basic cell, or representative volume element, (RVE), of the periodic composite at a macroscopic scale in order to obtain a solution. In the case of unidirectional fibrous composites, the following simplified assumptions are generally adopted:

i) The fibers are perfectly cylindrical in shape.

ii) All cross – sectional areas of the cylindrical model have the same microstructure.

iii) The matrix and the fibers are elastic, isotropic and homogenous and the fiber arrangement is uniform so that no agglomeration occurs.

In this investigation, we shall attempt to predict the fiber distribution inside the matrix introducing three geometric models.

Let us initiate our analysis presenting a triangular prismatic model appearing in Fig.1

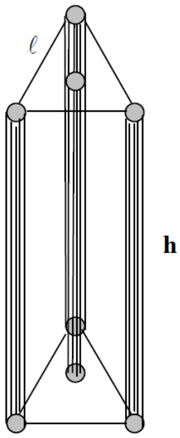

Fig. 1 Triangular prismatic model

Here, we point out that the fibers surround the vertices and the centroid axis of a triangular prism of edge ℓ and height h. Next, to create a unit cell capable to simulate unidirectional fibrous composites of periodic structure we consider a second prism of side 2ℓ such that to circumscribe the first one, as it can be seen in Fig. 2

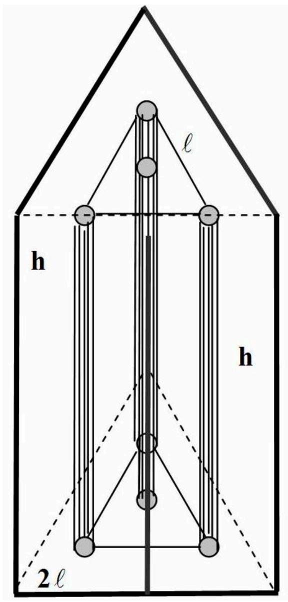

Fig. 2 Triangular prismatic RVE

The above unit cell is reproduced in space in a symmetrical manner and therefore it can describe a periodic, unidirectional fibrous composite of ideal fibers. Then to facilitate our investigation, we may transform the above microstructural model into a 4 – phase cylindrical model consisting of four concentric cylinders of radii a, b, c, d respectively such that a<b<c<d. The cross – sectional area of this model is illustrated in Fig. 3

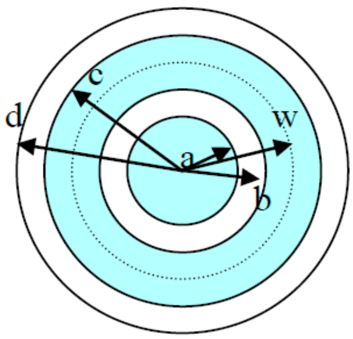

Fig. 3 Four – phase cylindrical model

Evidently, the second and fourth phase, (the cylindrical region of inner radius a, and outer radius b and the cylindrical region of inner radius c and outer radius d), represent the matrix.
Also, the central cylinder of radius a, i.e. the first phase, together with the cylindrical region of inner radius b and outer one c, i.e. the third phase, represent the fibers.

On the other hand, it is known from Euclidean Geometry that the volume of a triangular prism of edge 2ℓ is given as

$$V = (2\ell)^2 \cdot \frac{\sqrt{3}}{4} \cdot h \Rightarrow V = \sqrt{3}\,\ell^2 \cdot h \tag{1}$$

Besides, the fiber volume fraction U_f is estimated as

$$U_f = \frac{3\pi \cdot r_f^{\,2} \cdot h + \pi r_f^{\,2} h}{\sqrt{3}\,\ell^2 \cdot h} \tag{2}$$

and therefore

$$\ell = r_f \sqrt{\frac{4\pi}{\sqrt{3} \cdot U_f}} \tag{3}$$

According to our proposed geometric transformation, the volume of a triangular prism of edge 2ℓ reduces to the volume of a cylinder of radius d. Hence one infers

$$\sqrt{3}\lambda^2 \cdot h = \pi d^2 \cdot h \Rightarrow d = 2\ell \sqrt{\frac{\sqrt{3}}{\pi}} \Rightarrow$$

$$d = r_f \sqrt{\frac{4}{U_f}} \tag{4}$$

Also, since it is evident that the first phase of the cylindrical model [Fig. 3] encircles the centroid axis of the triangular prism it follows

$$a = r_f \tag{5}$$

Moreover, in the prism of Fig. 1 let w be the distance between the centroid axis and each vertex. Hence, the following relationship holds

$$w = \ell \cdot \frac{\sqrt{3}}{3} \tag{6}$$

Here, without violating our proposed formalism, let us also assume that in the 4 – phase model occurring in Fig. 3 the circle of radius w, drawn by dotted line, lies in the middle of the circular section which denotes the third phase.
Thus, the following relationships imply

$$c - w = w - b \Rightarrow c = 2w - b \tag{7}$$

and

$$\pi(c^2 - b^2)h = 3\pi r_f^2 h \Rightarrow c^2 - b^2 = 3r_f^2 \tag{8}$$

Solving the above system for b and c respectively, one obtains

$$b = w - \frac{3r_f^{\,2}}{4w} \;;\; c = w + \frac{3r_f^{\,2}}{4w} \tag{9 a,b}$$

Moreover, the following geometric restrictions hold

$$b > a \;;\; d > c \tag{10 a,b}$$

The first restriction yields

$$b^2 > a^2 \Rightarrow \left(w - \frac{3}{4}\frac{r_f^2}{w} \right)^2 \geq r_f^2 \Rightarrow$$

$$\Rightarrow r_f^2 \leq \frac{3}{9} \cdot r_f^2 \frac{4\pi}{\sqrt{3}U_f} + \left(\frac{3}{4}\right)^2 \cdot \frac{r_f^2}{\frac{3}{9} \cdot \frac{4\pi}{\sqrt{3}U_f}} - 1.5 r_f^2 \Rightarrow$$

$$\left(\frac{3}{4}\right)^2 \cdot \frac{U_f^2}{\frac{3}{9} \cdot \frac{4\pi}{\sqrt{3}}} - 2.5U_f + \left(\frac{3}{9} \cdot \frac{4\pi}{\sqrt{3}}\right) \geq 0 \Rightarrow$$

$$U_f \leq 1.0748 \qquad (11)$$

Also, according to the second constraint it follows

$$d^2 > c^2 \Rightarrow r_f^2 \frac{4}{U_f} \geq \left(w + \frac{3}{4}\frac{r_f^2}{w} \right)^2 \Rightarrow$$

$$\Rightarrow r_f^2 \frac{4}{U_f} \geq \frac{3}{9} \cdot r_f^2 \frac{4\pi}{\sqrt{3}U_f} + \left(\frac{3}{4}\right)^2 \cdot \frac{r_f^2}{\frac{3}{9} \cdot \frac{4\pi}{\sqrt{3}U_f}} + 1.5 r_f^2 \Rightarrow$$

$$\left(\frac{3}{4}\right)^2 \cdot \frac{U_f^2}{\frac{3}{9} \cdot \frac{4\pi}{\sqrt{3}}} + 1.5U_f + \left(\frac{3}{9} \cdot \frac{4\pi}{\sqrt{3}} - 4\right) \leq 0 \Rightarrow$$

$$U_f \leq 0.9225 \qquad (12)$$

Hence the performed prismatic model transformed into a 4 – phase cylindrical model can be valid for $U_f \leq 92.25\%$

In continuing, let us consider the following square prismatic model [Fig.4]

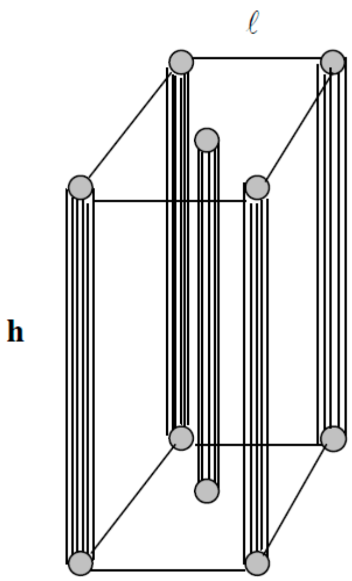

Fig.4 Square prismatic model

Following the same reasoning as before, we design the RVE below which obviously is able to simulate unidirectional fibrous composites of periodic structure [Fig.5].

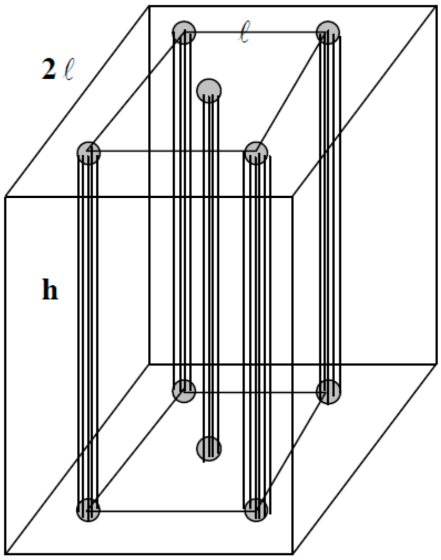

Fig.5 Square prismatic RVE

Next, to simplify our analysis utilizing the structural symmetries of the above model, we may transform it into the same 4 – phase cylindrical model, the cross – section of which first appeared in Fig.3 Meanwhile, the volume of a square prism of edge 2ℓ is given as

$$V = (2\ell)^2 \cdot \mathrm{h} \tag{13}$$

Furthermore, in this model the fiber content is evaluated as

$$\mathrm{U_f} = \frac{4\pi \cdot \mathrm{r_f}^2 \cdot \mathrm{h} + \pi \mathrm{r_f}^2 \mathrm{h}}{(2\ell)^2 \cdot \mathrm{h}} \tag{14}$$

and therefore

$$\ell = \mathrm{r_f} \sqrt{\frac{5\pi}{4 \cdot \mathrm{U_f}}} \tag{15}$$

Taking into account the proposed geometric transformation, the volume of a square prism of edge 2ℓ reduces again to the volume of a cylinder of radius d . Hence we infer

$$(2\ell)^2 \cdot \mathrm{h} = \pi \mathrm{d}^2 \cdot \mathrm{h} \Rightarrow \mathrm{d} = 2\ell \sqrt{\frac{1}{\pi}} \tag{16}$$

Eqn. (16) can be combined with eqn. (15) to yield

$$\mathrm{d} = \mathrm{r_f} \sqrt{\frac{5}{\mathrm{U_f}}} \tag{17}$$

In addition, it is obvious that the first phase of the cylindrical model [Fig. 3] should surround the centroid axis of the square prism and therefore the validity of eqn. (5) is also extended to the second prismatic model.

Now, in the square prism of Fig. 4 the distance w between the centroid axis and each vertex is given as

 doi:10.20944/preprints201705.0057.v1

$$w = \ell \frac{\sqrt{2}}{2} \tag{18}$$

Moreover, since we have already considered that in the 4 – phase model occurring in Fig. 3 the circle of radius w, lies in the middle of the circular section denoting the third phase, eqn. (7) still holds whereas eqn. (8), is replaced by

$$c^2 - b^2 = 4\,r_f^2 \tag{19}$$

Solving the system of eqns. (7) and (18) for b and c respectively, one obtains

$$b = w - \frac{4r_f^{\ 2}}{4w} \tag{20}$$

$$c = w + \frac{4r_f^{\ 2}}{4w} \tag{21}$$

Furthermore, the geometric constraints expressed by eqns. (10 a,b) hold for this model as well.
Now, the first restriction yields

$$b^2 > a^2 \Rightarrow w^2 + \frac{r_f^{\ 4}}{w^2} - 2r_f^{\ 2} \geq r_f^{\ 2} \Rightarrow$$

$$\frac{1}{2}\cdot r_f^{\ 2}\frac{5\pi}{4U_f} + \frac{r_f^{\ 4}}{\frac{1}{2}\cdot r_f^{\ 2}\frac{5\pi}{4U_f}} - 3r_f^{\ 2} \geq 0 \Rightarrow$$

$$\frac{1}{\frac{1}{2}\cdot\frac{5\pi}{4}}\cdot U_f^{\ 2} - 3U_f + \frac{1}{2}\cdot\frac{5\pi}{4} \geq 0 \Rightarrow$$

$$U_f \leq 0.7499 \tag{22}$$

Also, according to the second restriction we infer

$$d^2 > c^2 \Rightarrow r_f^{\ 2}\frac{5}{U_f} \geq \frac{2}{4}r_f^{\ 2}\frac{5\pi}{4U_f} + \frac{r_f^{\ 2}}{\frac{2}{4}\cdot\frac{5\pi}{4U_f}} + 2r_f^{\ 2} \Rightarrow$$

$$\frac{U_f^{\ 2}}{\frac{2}{4}\cdot\frac{5\pi}{4}} + 2U_f + \left(\frac{2}{4}\cdot\frac{5\pi}{4} - 5\right) \leq 0 \Rightarrow$$

$$U_f \leq 1.1698 \tag{23}$$

Thus, the second prismatic model is valid for $U_f \leq 74.99\%$.
Finally, let us present the following hexagonal prismatic microstructural model [Fig.6]

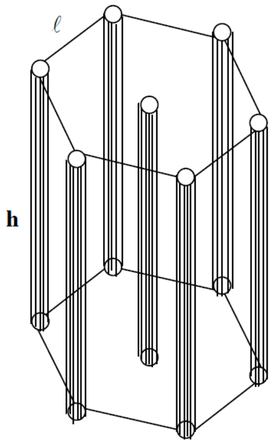

Fig. 6 Hexagonal prismatic model

Next, according to previous reasoning let us derive the following prismatic unit cell, the edge of which is now $\ell\sqrt{3}$ as it can be seen in Fig. 7

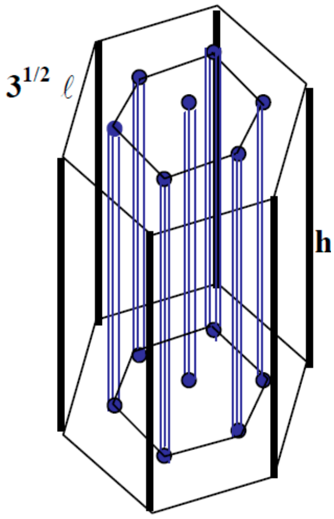

Fig.7 Hexagonal prismatic RVE

Then, to accommodate our analysis taking also into account the evident structural symmetries of the above hexagonal prismatic model, we may transform it again into the same 4 – phase cylindrical model of Fig. 3.

On the other hand, the volume of a hexagonal prism of edge $\ell\sqrt{3}$ given as

$$V = 3 \cdot \left(\sqrt{3}\ell\right)^2 \cdot \frac{\sqrt{3}}{2} \cdot h \Rightarrow V = \frac{9}{2}\ell^2\sqrt{3} \cdot h \quad (24)$$

Concurrently, the filler content is calculated as

$$U_f = \frac{6\pi \cdot r_f^{\ 2} \cdot h + \pi r_f^{\ 2} \cdot h}{\frac{9}{2}\sqrt{3} \cdot \lambda^2 \cdot h} \qquad (25)$$

and therefore

$$\ell = r_f \sqrt{\frac{7\pi}{4{,}5 \cdot \sqrt{3} \cdot U_f}} \qquad (26)$$

Taking into consideration the performed geometric transformation, the volume of a hexagonal prism of edge $\ell\sqrt{3}$ reduces to the volume of a cylinder of radius d.

Hence we deduce that

$$\frac{9}{2}\ell^2\sqrt{3}\cdot h = 2\pi d^2 h \Rightarrow d = \ell\sqrt{\frac{9\sqrt{3}}{2\pi}} \qquad (27)$$

Hence, the latter equation combined with (25) yields

$$d = r_f \sqrt{\frac{7}{U_f}} \qquad (28)$$

Evidently, the first phase of the cylindrical model of Fig. 3 should encircle the centroid axis of the hexagonal prism and therefore we deduce that the validity of eqn. (5) concerns the third model as well.

Besides, in the hexagonal prism of Fig. 6 the distance w between the centroid axis and each vertex is given as

$$w = \ell \qquad (29)$$

In addition, since we have supposed that in the 4 – phase model of Fig. 3 the circle of radius w, lies in the middle of the circular section denoting the third phase, eqn. (7) still holds while eqn. (8), is replaced by

$$c^2 - b^2 = 6\, r_f^2 \qquad (30)$$

The solution of the system of eqns. (7) and (29) for b, c respectively yields

$$b = w - \frac{6{r_f}^2}{4w} \qquad (31)$$

$$c = w + \frac{6{r_f}^2}{4w} \qquad (32)$$

Meanwhile, the geometric restrictions furnished by eqns. (10 a,b) are also valid for this model.

Here, the first constraint yields

$b^2 > a^2 \Rightarrow$

$${r_f}^2 \frac{7\pi}{4.5\sqrt{3}U_f} + \left(\frac{6}{4}\right)^2 \cdot \frac{{r_f}^2}{\frac{7\pi}{4.5\sqrt{3}U_f}} - 3{r_f}^2 \geq {r_f}^2 \Rightarrow \left(\frac{6}{4}\right)^2 \cdot \frac{{U_f}^2}{\frac{7\pi}{4.5\sqrt{3}}} - 4U_f + \frac{7\pi}{4.5\sqrt{3}} \geq 0 \Rightarrow$$

$$U_f \leq 0.8491 \qquad (33)$$

Also, according to the second constraint we find

Preprints (www.preprints.org) | NOT PEER-REVIEWED | Posted: 8 May 2017 doi:10.20944/preprints201705.0057.v1

$d^2 > c^2 \Rightarrow$

$$r_f^2 \frac{7}{U_f} \geq r_f^2 \frac{7\pi}{4{,}5\sqrt{3}U_f} + \left(\frac{6}{4}\right)^2 \cdot \frac{r_f^2}{\frac{7\pi}{4{,}5\sqrt{3}U_f}} + 3r_f^2 \Rightarrow \left(\frac{6}{4}\right)^2 \cdot \frac{U_f^2}{\frac{7\pi}{4{,}5\sqrt{3}}} + 3U_f + \left(\frac{7\pi}{4{,}5\sqrt{3}} - 7\right) \leq 0 \Rightarrow$$

$$U_f \leq 1.0818 \qquad (34)$$

Consequently, the third prismatic model is valid for $U_f \leq 84.91\%$

3. The concept of interphase – Towards a seven – phase cylindrical model

The reasons for introducing the concept of interphase in composite materials as well as proof that the introduction of this phase, yields results which are closer to real characteristic values of the composites are well established in Ref. [21]. Here, the concept of interphase will be taken into consideration together with the fiber arrangement and contiguity. In this context, the intermediate phase forms three cylindrical shells which surround the cylindrical fibers in the previously proposed prismatic models and thus it adds three more phases to the corresponding 4 – phase cylindrical model. Therefore, the final inhomogeneous cylindrical model according to which we shall estimate the thermal conductivities of the fibrous composite material will have seven distinguished phases, as it is illustrated in Fig. 8.

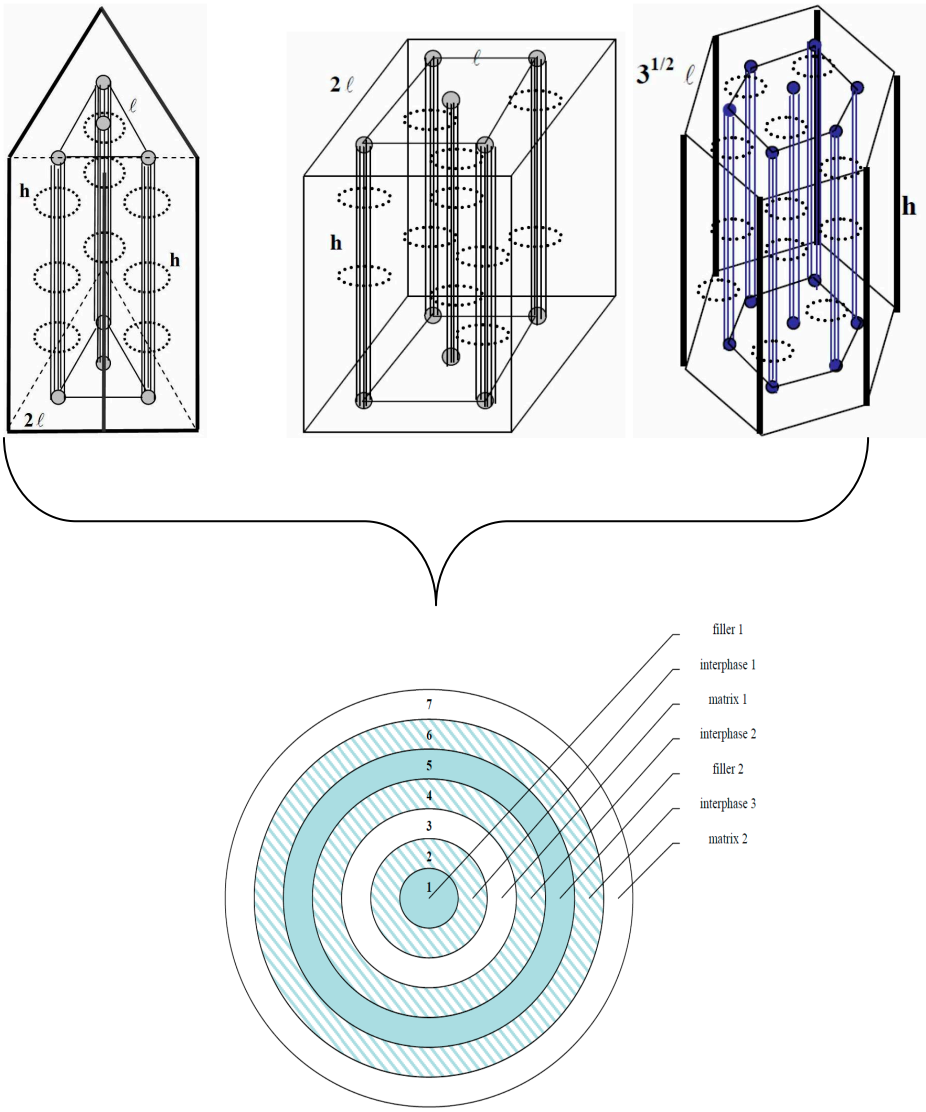

Fig. 8 Transformation of the three new unit cells into a 7 – phase cylindrical model

Preprints (www.preprints.org) | NOT PEER-REVIEWED | Posted: 8 May 2017 doi:10.20944/preprints201705.0057.v1

In the inhomogeneous new multiphase model, the first phase from inside to outside having radius r_1 represents the first area of the filler. The second phase is the cylindrical shell with the inner radius r_1 and outer radius r_2 and represents the first region of the intermediate phase. Also, the third phase is the cylindrical shell of inner radius r_2 and outer radius r_3 and shows the first region of the matrix. The fourth phase is the cylindrical shell with the inner radius r_3 and the outer radius r_4 and represents the second region of the intermediate phase. The fifth phase is the cylindrical shell of inner radius r_4 and outer radius r_5 and represents the second region of the filler. The sixth stage is the cylindrical shell of inner radius r_5 and outer radius r_6 representing the third region of the interphase. The seventh and last phase is the cylindrical shell with an inner radius r_6 and an outer radius r_7 and represents the second region of the matrix.
In continuing, we should determine the radii of the three interphases r_2, r_4, r_6 along with the interphase volume fractions in the three regions separately. To this end, let us adopt the following notations:

$$U_1 = U_{f,1}; U_2 = U_{i,1}; U_3 = U_{m,1}; U_4 = U_{i,2}; U_5 = U_{f,2}; U_6 = U_{i,3}; U_7 = U_{m,2}$$

Evidently the following relationships hold

$$U_f = U_1 + U_5; U_m = U_3 + U_7; U_i = U_2 + U_4 + U_6 \qquad (35\ a,b,c)$$

Moreover, given that the interphase is considered as somewhat an altered matrix and its proportion is constant wherever it can be developed, we infer

$$\frac{U_{i,1}+U_{i,2}}{U_{m,1}} = \frac{U_{i,3}}{U_{m,2}} = \frac{U_{i,1}+U_{i,2}+U_{i,3}}{U_{m,1}+U_{m,2}} = \frac{U_i}{U_m} = \frac{U_i}{1-U_f-U_i} = k \qquad (36)$$

where

$$U_m = 1 - U_f - U_i \qquad (37)$$

Also, without violating the generality, let us assume that

$$U_{i,1} = U_{i,2} \qquad (38)$$

Thus we obtain

$$\frac{U_{i,1}}{U_{m,1}} = k \Rightarrow U_{i,1} = kU_{m,1} \Rightarrow \frac{\pi\left(r_2^2 - r_1^2\right)h}{\pi d^2 h} = k\frac{\pi\left(r_3^2 - r_2^2\right)h}{\pi d^2 h} \Rightarrow \left(r_2^2 - r_1^2\right) = k\left(r_3^2 - r_2^2\right) \Rightarrow$$
$$(k+1)r_2^2 = kr_3^2 + r_1^2 \Rightarrow r_2^2 = \frac{kr_3^2 + r_1^2}{k+1} \Rightarrow r_2 = \sqrt{\frac{kr_3^2 + r_1^2}{k+1}} \qquad (39)$$

and

$$U_{i,2} = kU_{m,1} \Rightarrow \frac{\pi\left(r_4^2 - r_3^2\right)h}{\pi d^2 h} = k\frac{\pi\left(r_3^2 - r_2^2\right)}{\pi d^2 h} \Rightarrow \left(r_4^2 - r_3^2\right) = k\left(r_3^2 - r_2^2\right) \Rightarrow$$
$$r_4^2 = (k+1)r_3^2 - kr_2^2 \Rightarrow r_4 = \sqrt{(k+1)r_3^2 - kr_2^2} \qquad (40)$$

and

$$U_{i,3} = kU_{m,2} \Rightarrow \frac{\pi\left(r_6^2 - r_5^2\right)h}{\pi d^2 h} = k\frac{\pi\left(r_7^2 - r_6^2\right)}{\pi d^2 h} \Rightarrow \left(r_6^2 - r_5^2\right) = k\left(r_7^2 - r_6^2\right) \Rightarrow$$
$$\left(k+1\right)r_6^2 = kr_7^2 + r_5^2 \Rightarrow r_6^2 = \frac{kr_7^2 + r_5^2}{\left(k+1\right)} \Rightarrow r_6 = \sqrt{\frac{kr_7^2 + r_5^2}{\left(k+1\right)}} \qquad (41)$$

At this point, we should note that since the interphase is an altered matrix and thus there is no addition of other materials in our final model, the radii a,b,c,d of the 4 - phase model introduced in the previous Section, also appear in the proposed 7 – phase model and now have just been renamed as r_1 r_3 r_5 r_7 respectively. Hence, in the above relations we have expressed the interphase radii of the 7 – phase cylindrical model in terms of the radii b,c,d of the 4 – phase one, which does not contain any intermediate phase. Moreover, the outer radius of the 4 – phase model remains as is, after the development of the intermediate phase around the fiber. Also, the outer and inner radius of the filler phase in the 4 – phase model remains the same in the 7 – phase model. These results are attributed to the fact that the intermediate phase does not affect the volume in filler content, only the volume in matrix content. According to this viewpoint, we should also emphasize that all restrictions for filler content U_f arising from the geometric constraints of the prismatic models introduced in the previous Unit, i.e. inequalities (11), (12), (22), (23) also concern the new seven – phase model. In the sequel, one may evaluate the volume fractions of all phases in terms of the corresponding radii as follows

$$\begin{aligned}
U_1 &= U_{f,1} = \frac{\pi r_1^2 h}{\pi r_7^2 h} = \frac{r_1^2}{r_7^2} \\
U_2 &= U_{i,1} = \frac{\pi\left(r_2^2 - r_1^2\right)h}{\pi r_7^2 h} = \frac{\left(r_2^2 - r_1^2\right)}{r_7^2} \\
U_3 &= U_{m,1} = \frac{\pi\left(r_3^2 - r_2^2\right)h}{\pi r_7^2 h} = \frac{\left(r_3^2 - r_2^2\right)}{r_7^2} \\
U_4 &= U_{i,2} = \frac{\pi\left(r_4^2 - r_3^2\right)h}{\pi r_7^2 h} = \frac{\left(r_4^2 - r_3^2\right)}{r_7^2} \\
U_5 &= U_{f,2} = \frac{\pi\left(r_5^2 - r_4^2\right)h}{\pi r_7^2 h} = \frac{\left(r_5^2 - r_4^2\right)}{r_7^2} \\
U_6 &= U_{i,3} = \frac{\pi\left(r_6^2 - r_5^2\right)h}{\pi r_7^2 h} = \frac{\left(r_6^2 - r_5^2\right)}{r_7^2} \\
U_7 &= U_{m,2} = \frac{\pi\left(r_7^2 - r_6^2\right)h}{\pi r_7^2 h} = \frac{\left(r_7^2 - r_6^2\right)}{r_7^2} \qquad (42)
\end{aligned}$$

On the other hand, the fibrous composite material in reality consists of three different phases (matrix, fiber and interphase) and according to our model is divided in seven distinguished phases.
Lipatov [22] proved that, if calorimetric measurements are performed in the neighborhood of the glass transition zone of the composite, energy jumps are observed. These jumps are too sensitive to the amount of filler added to the matrix and can be used to evaluate the boundary layers developed around the filler. Apparently, as the filler volume fraction is increased, the proportion of macromolecules characterized by a reduced mobility is also increased. This is equivalent to an augmentation of the interphase content and supports the empirical conclusion presented in Ref. [22], that the extent of the interphase expressed by its thickness $\Delta r_i = r_i - r_f$, is the cause of the variation of the amplitudes of heat capacity jumps appearing at the glass transition zones of the matrix material and the composite with various filler – volume fractions. Moreover, the size of heat capacity jumps for unfilled and filled materials is directly related to Δr_i by an empirical relationship given in Ref. [22] and verified in Ref. [23]. This expression defines the interphase thickness and is given as

$$\frac{(r_{\mathrm{f}}+\Delta r_i)^3}{r_{\mathrm{f}}^3}-1=\frac{\lambda U_{\mathrm{f}}}{1-U_{\mathrm{f}}} \quad (43)$$

In addition the interphase volume fraction arises from the following expression

$$U_i=\frac{3U_{\mathrm{f}}\Delta r_i}{r_{\mathrm{f}}} \quad (44)$$

with $\lambda=1-\frac{\Delta C_p^f}{\Delta C_p^0}$ (45)

Here, the numerator and the denominator of the fraction appearing in the right member of Eqn. (32) are the sudden changes of the heat capacity for the filled and unfilled polymer respectively.
Also, according to our multiphase model, it is evident that

$$r_{\mathrm{i}}=\mathrm{r}_2+\mathrm{r}_4+\mathrm{r}_6 \quad (46)$$

Concurrently, it has been shown [21] that for the unidirectional fiber composites, the following parabolic relationship between the content of the intermediate phase and the filler content holds

$$U_i=C\cdot U_{\mathrm{f}}^2 \quad (47)$$

where C=0.123 [24]

Thus, for any ordered couple (U_f , U_i), by the use of eqns. (35 a,b,c) along with eqns. (36) to (45) one may calculate the radii of the seven – phase model, provided that the diameter of the cylindrical fibers is known.

4. Materials and Experimental Work

The unidirectional glass-fiber composites used in the experimental part of the our investigation consisted of an epoxy matrix (Permaglass XE5/ 1, Permali Ltd., U.K.) reinforced with long E-glass fibers. The matrix material was based on a diglycidyl ether of bisphenol A together with an aromatic amine hardener (Araldite MY 750/ HT972, Ciba – Geigy, U.K.). The glass fibers had a diameter of $1.2\cdot10^{-5}m$ and were contained at a volume fraction of about 65%. The fiber content was determined, as customary, by igniting samples of the composite and weighting the residue, which gave the weight fraction of glass as: $\mathrm{w}_{\mathrm{f}}=79.6\pm0.28\%$. This and the measured values of the relative densities of permaglass (p_f = 2.55 gr/cm^3) and of the epoxy matrix (p = 1.20 gr/cm^3) gave the value U_f = 0.65. Furthermore, chip specimens with a 0.004 m diameter and thicknesses varying between 0.001 and 0.0015 m made either of the fiber composite of different filler contents, or of the matrix material, were tested by the authors on a differential scanning calorimetry (DSC) Thermal Analyzer at the zone of the glass transition temperature for each mixture, in order to determine the specific heat capacity values.
More over, since the samples are discs of 4 mm in diameter and 1 mm in thickness it implies that their mass is about 50 mg.
Consequently, the results emerging from the proposed mathematical analysis along with the experimental data are summarized in Table 1, whereas Fig. 9 illustrates the variation of the overall interphase content of the composite versus the fiber volume fraction.

U_f	U_i	r_1(μm)	r_2(μm)	r_3(μm)	r_4(μm)	r_5(μm)	r_6(μm)	r_7(μm)
0.10	0.0012	6	6.066	25.19	25.21	27.9	27.926	42.426
0.20	0.00492	6	6.124	16.77	16.82	20.62	20.692	30
0.30	0.01107	6	6.166	12.79	12.87	17.54	17.667	24.495
0.40	0.01968	6	6.185	10.23	10.34	15.77	15.976	21.213
0.50	0.03075	6	6.168	8.325	8.447	14.6	14.91	18.974
0.60	0.04428	6	6.089	6.764	6.843	13.77	14.211	17.321
0.65	0.052	6	6.009	6.057	6.066	13.44	13.964	16.641

Table 1. Radii of the seven – phase cylindrical model versus filler content

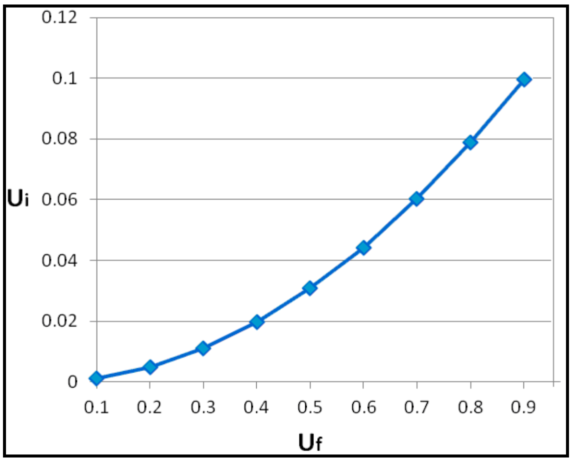

Fig. 9. Interphase content versus filler content

Next, in Table 2 we present the concentrated values of volume fractions for the seven phases with respect to filler content. Here, we elucidate that the geometrical constraints found in the previous Unit were taken into account.

U_1	U_2	U_3	U_4	U_5	U_6	U_7
0.02	0.00044	0.33206	0.00044	0.07956	0.00076	0.56674
0.04	0.00168	0.27082	0.00168	0.15832	0.00324	0.52426
0.06	0.00336	0.20914	0.00336	0.23664	0.00771	0.47979
0.08	0.00500	0.14750	0.00500	0.31500	0.01468	0.43282
0.10	0.00569	0.08681	0.00569	0.39431	0.02506	0.38244
0.12	0.00360	0.02890	0.00360	0.47640	0.04068	0.32682
0.13	0.00037	0.00213	0.00037	0.51963	0.05163	0.29587

Table 2. Volume fractions of all phases

5. Estimation of thermal conductivities

As we have emphasized, the concept of interphase has been considered together with the influence of fiber contiguity on the themomechanical properties of the composite.
Generally, the coefficient of thermal conductivity of this intermediate phase K_i can be expressed as an n – degree polynomial with respect to the radius r.
To cover the whole spectrum of variation of the quantity K_i, let us suppose five different approaches:

a) Linear Variation

The first approach is a linear variation of the thermal conductivity of the interphase K_i with respect to radius r.

$$\mathrm{K}_i(r) = A + B \cdot r \tag{48}$$

where A and B are quantities varying with respect to the radii of matrix and fiber.

To evaluate these terms, we should take into consideration the following boundary conditions.

$$r = r_\mathrm{f} \Rightarrow \mathrm{K}_i(r) = \eta \mathrm{K}_\mathrm{f}$$

$$r = r_i \Rightarrow \mathrm{K}_i(r) = \mathrm{K}_m(r) \tag{49 a,b}$$

At $r_\mathrm{f} \le r \le r_i$

Here, we have assumed that the coefficient of thermal conductivity of the interphase, at the boundary with the matrix, coincides with the quantity K_m.
Besides, at the interface between first interphase and filler, the quantity K_i constitutes actually a portion of K_f, which implies that $\mathrm{K}_i < \mathrm{K}_\mathrm{f}$.
This influence is described by the indicator η the rates of which belong to the interval $(0,1]$. Hence the following relationship arises

$$\mathrm{K}_i(r) = \frac{\eta \mathrm{K}_\mathrm{f}(r_i - r) + \mathrm{K}_m(r - r_\mathrm{f})}{(r_i - r_\mathrm{f})} \tag{50}$$

b) Parabolic Variation

Next, let us assume a parabolic variation of thermal conductivity with respect to the radius r:

Hence the following equality holds:

$$\mathrm{K}_i(r) = Ar^2 + Br + C \tag{51}$$

$$r_\mathrm{f} \le r \le r_i$$

To estimate the terms A, B and C which depend on the radii as well as the thermal conductivities of constituents of the composite, we can also apply the previous boundary conditions.
In addition, one may suppose that all the parabolas which represent graphically this aforementioned variation should have global minima at the critical values r_i . The corresponding mathematical expression of this requirement, can be formulated as follows
At $r = r_i$

$$\frac{d\mathrm{K}_i}{dr} = 0\,;\ \frac{d^2\mathrm{K}_i}{dr^2} > 0 \tag{52}$$

Therefore, after the necessary algebraic manipulation, the following relationship arises

$$K_i(r)=\frac{(\eta\cdot K_f-K_m)(r-2r_i)r+\eta\cdot K_f r_i^2+K_m\cdot r_f^2-2\eta\cdot K_m r_f r_i}{(r_i-r_f)^2} \tag{53}$$

c) Hyperbolic Variation

In continuing, we assume a hyperbolic variation for $K_i(r)$ as expressed by the following formula

$$K_i(r)=A+\frac{B}{r} \tag{54}$$

when $r_f \le r \le r_i$

To calculate the quantities A and B we may use the same boundary conditions. Thus, it follows:

$$K_i(r)=\frac{K_m r_i-\eta K_f r_f}{r_i-r_f}+\frac{(\eta K_f-K_m)r_f r_i(r-2r_i)}{(r_i-r_f)r} \tag{55}$$

d) Logarithmic Variation

According to a logarithmic variation, the term $K_i(r)$ emerges from the following expression:

$$K_i(r)=A\ln\frac{B}{r} \tag{56}$$

$r_f \le r \le r_i$

By taking into account the same boundary conditions as previously, we obtain

$$K_i(r)=\frac{\eta K_f-K_m}{\ln\frac{r_i}{r_f}}\ln\frac{r_i^{\eta K_f/(\eta K_f-K_m)}}{r\cdot r_i^{\eta K_m/(\eta K_f-K_m)}} \tag{57}$$

e) Exponential Variation

Finally, let us suppose that the quantity $K_i(r)$ varies according to a generic exponential law in the following form

$$K_i(r)=A\cdot e^{Br} \tag{58}$$

An application of the same boundary conditions as previously yields

$$K_i(r)=\frac{\eta K_f}{\ln\left(\frac{K_m}{\eta K_f}\right)}e^{\frac{\ln\frac{K_m}{\eta K_f}}{r_i-r_f}r} \tag{59}$$

The coefficient of longitudinal thermal conductivity, according to a modified form of the standard law of mixtures, which arises from our proposed multiphase model, is given as

$$K_{Lc}=K_f(U_{f,1}+U_{f,2})+K_m(U_{m,1}+U_{m,2})+K_i(U_{i,1}+U_{i,2}+U_{i,3}) \Leftrightarrow$$

$$K_{Lc}=K_f\left(\frac{r_1^2+r_5^2-r_4^2}{r_7^3}\right)+K_m\left(\frac{r_3^2-r_2^2+r_7^2-r_6^2}{r_7^2}\right)+K_i\left(\frac{r_2^2-r_1^2+r_4^2-r_3^2+r_6^2-r_5^2}{r_7^2}\right)\Leftrightarrow$$

$$\mathrm{K}_{Lc} = \mathrm{K}_f\left(\frac{r_1^2 + r_5^2 - r_4^2}{r_7^3}\right) + \mathrm{K}_m\left(1 + \frac{r_3^2 - r_2^2 - r_6^2}{r_7^2}\right) + \mathrm{K}_i\left(\frac{r_2^2 - r_1^2 + r_4^2 - r_3^2 + r_6^2 - r_5^2}{r_7^2}\right) \tag{60}$$

where $\mathrm{K}_{Lc}, \mathrm{K}_f, \mathrm{K}_m$ denote the thermal conductivities of composite, filler and matrix respectively.

In continuing, according to a modified form of the inverse law of mixtures, which also emerges with the aid of the same model, one obtains the following relationship for the transverse thermal conductivity K_{Tc}.

$$\frac{1}{\mathrm{K}_{Tc}} = \frac{\dfrac{r_1^2 + r_5^2 - r_4^2}{r_7^3}}{\mathrm{K}_f} + \frac{1 + \dfrac{r_3^2 - r_2^2 - r_6^2}{r_7^2}}{\mathrm{K}_m} + \frac{\dfrac{r_2^2 - r_1^2 + r_4^2 - r_3^2 + r_6^2 - r_5^2}{r_7^2}}{\mathrm{K}_i(r)} \tag{61}$$

Solving eqn. (61) for K_{Tc} we obtain

$$\mathrm{K}_{Tc} = \frac{\mathrm{K}_f \mathrm{K}_m \mathrm{K}_i}{\mathrm{K}_m \mathrm{K}_i\left(\dfrac{r_1^2 + r_5^2 - r_4^2}{r_7^3}\right) + \mathrm{K}_f \mathrm{K}_i\left(1 + \dfrac{r_3^2 - r_2^2 - r_6^2}{r_7^2}\right) + \mathrm{K}_f \mathrm{K}_m\left(\dfrac{r_2^2 - r_1^2 + r_4^2 - r_3^2 + r_6^2 - r_5^2}{r_7^2}\right)} \tag{62}$$

6. Discussion

In the previously presented qualitative analysis towards the estimation of thermal conductivities for periodic fibrous composites, the entire material was assumed beforehand to be inhomogeneous. The thermal field was examined by the use of fiber arrangement and an inhomogeneous interphase region that was developed around each fiber. Next the coefficients $\mathrm{K_L}$ and $\mathrm{K_T}$ were estimated via modified forms of standard and inverse law of mixtures respectively.

An endeavor was made by the authors to amend these laws in a unified manner by consider the influence of internal and neighbouring fibers via deterministic configurations along with the interphase concept.

In this context, according to the proposed prismatic models three different periodic stacking of fibers encircled with inhomogeneous interphase layers were transformed into a 7 – phase cylindrical mode in a unified manner.

This transformation is based entirely on the equality of volume fractions between each distinct phase of the prismatic models with their corresponding phase in the multilayer cylindrical model.

Here one could remark that the transformation of a prismatic model into a multilayer cylindrical one has mainly to do with the application of Classical Elasticity approach to predict properties of fibrous composite materials, like elastic moduli, thermal expansion coefficients etc. Nevertheless, since the coefficient of thermal conductivity is a bulk property of materials one may note that such a topological transformation is not needed. Yet, thermal conductivity of filled polymers is proved to be analogous to viscosity, tensile modulus, and shear modulus. The following equation [25] demonstrates the numerical relationship between composite material and pure polymer:

$$\frac{k_c}{k_p} = \frac{n_c}{n_p} = \frac{\mathrm{E}_c}{\mathrm{E}_p} = \frac{G_c}{G_p} \tag{63}$$

where the subscripts "c" and "p" denote the composite and pure polymer property respectively.

Also, in the above equation the symbol "k" is used to denote thermal conductivity, "n" to denote viscosity, "E" for the elastic modulus, and "G" for the shear modulus. Besides, a shear loading analogy method was proposed by Springer and Tsai [26], to estimate thermal conductivity of a composite.

Nonetheless, since in many formulae predicting the properties of composites there are limitations concerning the values of filler content, it is our belief that the aforementioned topological transformation of the prismatic models into a multiphase cylindrical one is useful to take place in order to estimate the thermal conductivity, since in this way the analogy given by the previous relation may be signified and examined in a unified framework, when necessary. Moreover, in regard to the possible interaction amongst fibres which is motivated by the proposed configurations of them, indeed one may pinpoint that this is not in consensus with the concurrent use of mixing laws. However, we elucidate that in our case this interaction has not a quantitative character.

In particular, according to such geometric the fiber distribution inside the polymer matrix is carried out by means of deterministic configurations. In this way, the range of fiber vicinity is defined beforehand in a stringent manner. Hence, given that the development of interphase layers around all fibers is a fact that cannot be avoided especially in polymer composites filled with inorganic filler; our consideration is in opposition with the undesirable existence of consecutive or intersecting and thus interacting inhomogeneous interphase layers with evidently unspecified thicknesses. Besides, such an unexpected condition may also shift the optimum fiber volume fraction above which the reinforcing action of the fibers is upset. In our concept, any interphase region is developed solely around each fiber (internal or neighboring) and its thickness cannot be affected by the interphase layers of neighboring fibers and thus the rule of mixtures can be implemented as if an interphase layer to be developed around the central fiber and besides a “unique interphase layer” to be developed around a “unique equivalent neighboring fiber”. This standpoint can be extended to fibrous composites of higher filler contents, allowing us to combine the three basic prismatic models in order to create more advanced and complicated body or non body centered prismatic unit cells.

Hence, the fiber configurations contribute to the thermal properties for periodic composites with prismatic arrangements as justified by the transformation of the introduced prismatic unit cells into a 7 – phase cylindrical model. This model has merged the influence of fiber distribution and the concept of interphase.

In this context, the longitudinal and transverse thermal conductivity of this class of periodic composites were obtained by exploring the combined effects of these two significant influential factors, something that can be also pointed out from the corresponding explicit expressions (60) and (62). Nevertheless, a shortcoming of our model is its weakness to predict the influence of any misalignments in the fiber orientation, something that may cause a local agglomeration amongst the fibers.

On the other hand, from Table 1 it is clear that the variables Δr_i and U_i are generally strictly increasing continuous functions at least up to a certain value of the fiber volume fraction. This type of variation is consistent with the fact that, due to the existence of fibers, a part of macromolecules which are in the close vicinity of the fiber surface, i.e. within the interphase region, are characterized by a reduced mobility. As a result of this type of behaviour of such macromolecules, the higher the fiber content, the larger fiber surface and, consequently, the higher amount of macromolecules with reducing mobility are developed in the matrix material.

In addition, eqns. (49) to (59) could be simplified if one considers that the influence of interphase is maximum and therefore the coefficient η becomes equal to unity.

Finally, it could be mentioned that although our samples the preparation of which was described in Unit 5 are very small, it is the authors’ opinion that are they representative of the composite medium at mesoscale due two the periodic microstructure of the overall material.

7. Conclusions

A multiphase model was performed to simulate the microstructure of periodic fibrous composites, and in sequel to estimate the longitudinal and transverse thermal conductivities. Apparently, the overall material was supposed to be inhomogeneous.

The novelty of this work was that the fiber contiguity was taken into consideration in parallel with the concept of interphase in order to evaluate these properties.

Moreover, according to the constraints for the filler content that we derived, it implies that the proposed model is not valid only for medium or low values of fiber volume fractions, given that their maximum value is generally 60%-70%.

 doi:10.20944/preprints201705.0057.v1

In closing, it can be said that the performed theoretical results, regardless of their qualitative character, may be considered as basic ones for more advanced cell models of unidirectional fibrous composites of periodic structure.

References

1) Papanicolaou, G. C., Paipetis, S. A., Theocaris, P. S.: The Concept of Boundary Interphase in Composite Mechanics, Kolloid Zeit. und Zeit. fUr Polymere 256, (7), pp. 625-630, (1978)

2) Theocaris, P. S., Papanicolaou, G. C.: The Effect of the Boundary Interphase on the Thermomechanical Behaviour of Composites Reinforced with Short Fibers, J. Fibre Sci. and Techn. 12 (6), pp. 421-433, (1979)

3) Papanicolaou,G.C., Theocaris,P.S., Spathis, G.D.: Adhesion Efficiency Between Phases in Fiber-Reinforced Polymers by Means of the Concept of Boundary Interphase, Col. and Polym. Sci. 258, pp. 1231-1237, (1980)

4) Kanaun, S.K. and Kudriavtseva, L.T. Spherically layered inclusions in a homogeneous elastic medium, Appl. Math. Mech., 50, 483-491, (1983).

5) Kanaun, S.K. and Kudriavtseva, L.T. Elastic and thermoelastic characteristics of composites reinforced with unidirectional fibre layers. Appl. Math. Mech., 53, 628-636 (1986).

6) Garboczi, E. J. and Bentz D. P. (1997) Analytical formulas for interfacial transition zone properties, Advanced Cement – Based Materials 6, 99-108.

7) Garboczi, E. J. and Berryman, J. G. (2000) New effective medium theory for the diffusivity or conductivity of a multi-scale concrete microstructure model, Conc. Sci. and Engin., 2, 88-96.

8) Lutz, M.P. and Zimmerman, R.W. (1996) Thermal stresses and effective thermal expansion coefficient of a functionally graded sphere. Journal of Thermal Stresses, 19, 39-54.

9) Lutz, M.P. and Zimmerman, R.W. (1996) Effect of the interphase zone on the bulk modulus of a particulate composite, Journal of Applied Mechanics, 63, 855-861.

10) Lutz, M.P. and Zimmerman, R.W. (2005) Effect of an inhomogeneous interphase zone on the bulk modulus and conductivity of a particulate composite, International Journal of Solids and Structures, 42, 429-437.

11) Shen, L and Li, J. (2003) Effective elastic moduli of composites reinforced by particle or fiber with an inhomogeneous interface, International Journal of Solids and Structures, 40, 1393-1409.

12) Sevostianov, I. Dependence of the effective thermal pressure coefficient of a particulate composite on particles size, International Journal of Fracture 145, 2007, 333-340.

13) Sevostianov, I. and Kachanov, M. Homogenization of a nanoparticle with graded interface. International Journal of Fracture 139, 2006, 121-127. International Journal of Engineering Science

14) E. Sideridis, V. Kytopoulos, G. Papadopoulos and G. Bourkas Influence of Low filler content on some thermomechanical properties of particulate epoxy composites simulated by a variant tetra-phase model Plastics, Rubber and Comp., Macromolecular Eng., Vol. 32, 6, p. 271 (2003).

15) E. Sideridis, V. Kytopoulos, E. Kyriazi and G. Bourkas Determination of Thermal Expansion Coefficient of Particulate Composites by the Use of a Triphase Model Comp. Sci. and Tech., Vol. 65, p. 909 (2005).

16) Barbero, Ever J. Introduction to Composite Materials Design, Taylor & Francis, 1998.

17) Nielsen L. E. The Thermal and Electrical Conductivity of Two-Phase Systems I & EC Fundamentals, Vol. 13, No. 1, pp. 17-30, 1974.

18) Z. Hashin Analysis of Properties of Fiber Composites With Anisotropic Constituents, J. Appl. Mech. 46 No. 3, 543-550 (1979)

19) Rodrigo P. A. Rocha, M Anuel, E. Cruz Computation of the effective thermal conductivity of unidirectional fibrous composites with an interfacial thermal resistance Numerical Heat Transfer, Part A: Applications Volume 39, Issue 2, pages 179-203 2001

20) J. Venetis, E. Sideridis, A mathematical model for thermal conductivity of homogeneous composite materials, Indian Journal of Pure & Applied Physics Vol. 54, May 2016, pp. 313-320

21) P. S. Theocaris, The Mesophase Concept in Composites, Polymers - Properties and Applications, Volume 11 (1987), Springer, Editors Dr. G. Henrici-Olivé, Prof. S. Olivé
ISBN: 978-3-642-70184-9 (Print) 978-3-642-70182-5

22) Lipatov Y. S.: Physical Chemistry of Filled Polymers, published by Khimiya (Moscow 1977). Translated from the Russian by R. J. Moseley, International Polymer Science and Technology, Monograph No.2; see also Lipatov, Y. S., Adv. Polym. Sci. 22, pp. I-59, (1977)

23) Theocaris, P. S., Papanicolaou G.C. Sideridis, E. Structural integrity studies in particulate composites by means of thermal capacity measurements. Jnl. of Reinforced Plastics and Composites, Vol.1, p. 92 (1982)

24) Theocaris, P. S., Sideridis, E. P., Papanicolaou, G. C.: The Elastic Longitudinal Modulus and Poisson's Ratio of Fiber Composites, J. Reinf. Plast. and Comp. 4 (4), pp. 396-418 (1985)

25) D. M. Bigg, Thermally Conductive Polymer Compositions. Polymer Composites, Vol. 7, No. 3, 1986, pp. 125.

26) Springer, G.S, Tsai S. W. Jnl. Comp. Mat., 1, pp. 166-173 (1967)